JOURNAL OF APPLIED ELECTROCHEMISTRY 21 (1991) 774–780

Electrochemical and reflectance study of the conversion of zinc oxide by hexacyanoferrate(II) in offset lithography
Part I: Zinc electrochemistry with minor components

D. R. ROSSEINSKY, J. D. SLOCOMBE, A. M. SOUTAR
Department of Chemistry, The University, Exeter EX4 4QD, UK

Received 19 September 1990; revised 16 January 1991

Electrophotographic ZnO undergoes special reactions at pH 4.6 with ferrocyanide and other, minor, solutes during pre-printing 'conversion'. Electrochemically produced ZnO on Zn can be used in monitoring the reactions, and in this paper the basic interactions of such ZnO (or hydroxide) with all the minor constituents apart from ferrocyanide are studied by cyclic voltammetry. The pre-treatment of the Zn metal affects the nature of the oxide/hydroxide film. Scans from -1.4 V (with respect to SCE) to -0.9 V show that small 'forward' (negative to positive) features are important, especially a minute current step, and the onset point of anodic current flow, before gross anodic dissolution. In the 'reverse' limb the major features (not occurring in all solution compositions) are reductions at ~ -1.15 V and at ~ -1.3 V, ascribed from observed dependences to Zn^{2+} reduction and oxide/hydroxide reduction respectively, though the variability of the oxide/hydroxide film limits reproducibility of the features. The effects of O_2, of NaH_2PO_4, of EDTA, of malic acid, surfactant and humectant on these features are studied, for an internally consistent account of the reactions.

1. Introduction

In offset lithography, a polymer image, produced by standard electrophotographic methods [1] on the surface of a polycrystalline zinc oxide 'plate', acquires the printing ink prior to its impression on the page. The plate comprises zinc oxide plus photosensitiser in a resin binder coated on to a paper base. The reaction of an oxide layer, electrochemically generated on a zinc electrode, with ferrocyanide and phosphate anions in solution, is used as a model to study the 'conversion' reaction [2, 3] by which the surface of the zinc oxide plate is transformed to a bulky hydrophilic layer by treatment with ferrocyanide-based solution, in order to prevent ink from adhering to the plate in the *non-image* areas by attachment to resin binder in the plate surface: the bulky hydrophilic material bridges over resin otherwise accessible to the ink.

The oxide film on zinc [4–9] has properties found to be highly dependent on pH. In alkali a passivating layer is formed, the mechanism of formation and composition of which are subject to debate [7–13]. In neutral perchlorate solution, Hamnett and Mortimer [4] report the formation of a non-passivating monolayer film of ZnO during cyclic voltammetry in the potential region -1.3 V to -1.2 V with respect to SCE, through which dissolution of the electrode occurs at more positive potentials. A number of different forms of film are possible: α-$Zn(OH)_2$, β-$Zn(OH)_2$, θ-$Zn(OH)_2$, γ-$Zn(OH)_2$, $Zn(OH)_{2(amorphous)}$, and the active and inactive forms of ZnO, ZnO_{act} and ZnO_{inact} [4]. We refer to any of these forms subsequently as Zn^{II} oxide.

Complex impedance [5–7] yields mechanistic data for both Zn^{2+} evolution and deposition: competitive processes in deposition involve the participation of adsorbed H together with Zn^{I} and Zn^{II} species [16], whereas only two undefined Zn species are inferred from an analysis [7], aimed at parametric conciseness, of the dissolution in sulphate medium. The solutions used here differ markedly from our electrophotographic media, especially in pH: at pH 3.8 and 5.8 in perchlorate, impedance studies [5] show only charge-transfer rate control plus diffusion control at low frequency, while the double layer capacitance indicates oxide film formation (without pre-adsorption of OH^-) at pH 5.8, whereas at pH 3.8 this probe gives no evidence of film formation. Such composition sensitivity shows the need for study of solutions at pH 4.6, the pH typical of technical conversion solutions; furthermore, the Zn response in the *absence* of ferrocyanide is clearly required.

Thus at pH 4.6, cyclic voltammetry of zinc metal from -1.4 V to -0.7 V with respect to SCE has now been used (Part I) to study the effect of the individual components of industrial conversion solution on the properties of an electrochemically generated zinc oxide layer on zinc in perchlorate background electrolyte; the effect of hexacyanoferrate(II) is dealt with in Part 2. Both aerated and deoxygenated electrolytes

0021-891X/91 $03.00 + .12

were used, following necessary precathodization at -1.4 V [4].

2. Experimental details

Voltammetry at 25° C was carried out in a standard two-compartment glass electrochemical cell, using aqueous (deionised water) 0.2 M $LiClO_4$ as background electrolyte in such excess as to swamp out effects on ionic strength of the minor changes made in other ionic solutes. pH was made to 4.6 with dilute $NaOH/HClO_4$. The working electrode comprised a $5 \times 5\,mm^2$ flag of polycrystalline zinc foil (Goodfellows 99.99% or greater purity) with a tag soldered to a length of tinned copper wire housed in a glass tube sealed at the tag with epoxy. Platinum wire counter and SCE reference electrodes were used.

Immersion of the Zn in concentrated HNO_3 to vigorous effervescence, then a thorough deionised water rinse and wet transfer to the cell was followed by one of these pretreatments, Fig. 1 showing consequent CVs: (i) short precathodisation, that is, cathodising at -1.4 V for 20 min with N_2 gas bubbling, Fig. 1a; (ii) long precathodisation, that is, as (i), but for 60 min, Fig. 1b,c; (iii) short (20 min only) cathodisation without N_2 at -1.4 V, of air-exposed electrolyte, Fig. 1d.

A PAR 174A potentiostat was used with an Advance Bryans Series-5000 X-Y two-pen recorder. Since a wide variety of compositions required study, one slow scan rate, 2 mV s^{-1}, was chosen in order to encompass all, especially the slow, steps; marginal variability of repeated scans disfavours scan-rate studies. To define

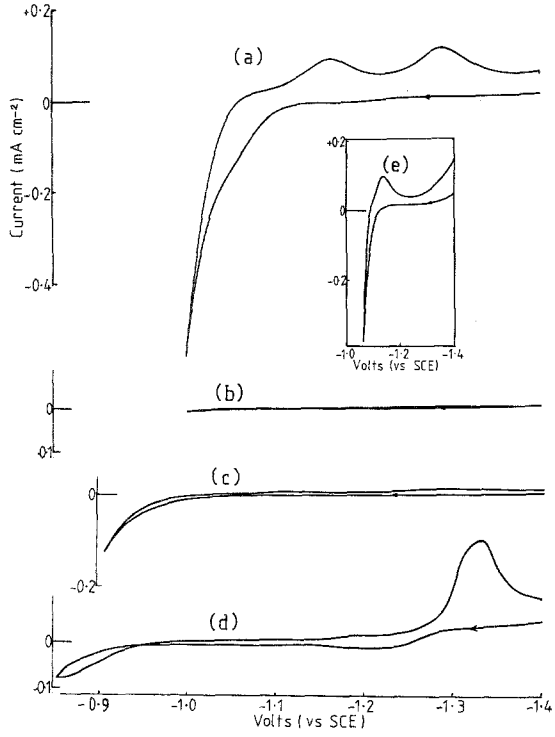

Fig. 1. CVs recorded in 0.2 M $LiClO_4$ (except e): (a) short precathodisation. Sweep reversed at -1.0 V; (b) long precathodisation. Sweep reversed at -1.0 V; (c) as (b) except sweep reversed at -0.9 V: reverse peaks enhanced; (d) short precathodization without deoxygenation. Sweep reversed at -0.85 V; and (e) 0.2 M NH_4ClO_4 in the place of $LiClO_4$ (60 min precathodised).

terminology, all CVs initially proceed from more to less negative potential (the 'forward' direction) before reversal (into the 'reverse' direction), unless otherwise stated.

In reflectance studies [8] a 12 V, 100 W tungsten-halogen lamp output (low intensity, to preclude photoelectrochemistry [6]) was partially focussed on the electrode surface, the reflected intensity being led by optical fibre, mounted close to the electrode surface, to a photodiode, the output via an operational amplifier being recorded as a function of applied potential to give a cyclic 'reflectogram' with the CV.

3. Results and discussion

Possible anodic reactions are: oxidation of the electrode material itself to give either zinc ions by dissolution [4] or zinc oxide/hydroxide, in the variety of different forms noted above. Hence the complex responses reported below are governed by the formation of ZnO films of varying structure.

The possible cathodic reactions are: deposition of zinc ions [4], reduction of ZnO [4], reduction of hydrogen ions [16] and, in aerated solution, the reduction of dissolved oxygen [6]. During -1.4 V precathodisation, the reduction of H^+ ion, and of O_2 in unpurged solution, occur. The current decreased steadily with time, and on subsequent cycling of the electrode, variable voltammetry was observed, dependent on the length of precathodization and on $[O_2]$. Longer precathodization (60 min) in deoxygenated electrolyte gave best reproducibility, both of peak size and peak potential.

3.1. *Precathodisation, and CV dependence on background electrolyte*

Oxygen-free pretreatments (60 min) led to CVs with the following features (the corresponding 20 min cathodic outcome being italicised) (Fig. 1): (a) a small forward cathodic current $\sim 10\,\mu A\,cm^{-2}$ ($\sim 20\,\mu A\,cm^{-2}$); (b) a small step decrease, over -1.2 V to -1.1 V (clearly evident with greater current sensitivity) (*-1.25 V to -1.16 V*) to a passivated plateau of very small current; (c) anodic-current onset between -1.04 and -1.00 V (*beyond -1.12 V*); (d) on reversal at potential less negative than -1.0 V, peaks centred at -1.15 and -1.3 V are observed, reversal at -1.0 V showing only a -1.3 V plateau, some anodic current being essential to any appearance of the reverse -1.15 V peak at all. The former peak is only moderately increased by increase of net (prior) anodic charge passed, the latter more so, the potentials of either being within the range ± 0.02 V (*± 0.04 V at -1.15 V, ± 0.03 V at -1.3 V, the latter peak sometimes showing extra, small, shoulders either side*).

The oxygen-containing solutions showed initial currents of $\sim 50\,\mu A\,cm^{-2}$, a step between -1.28 and -1.20 V (Fig. 1d), only a minute current to ~ -0.95 V, then slow anodic-current growth; on reversal cathodic peaks of variable size occur at ~ -1.18 V and

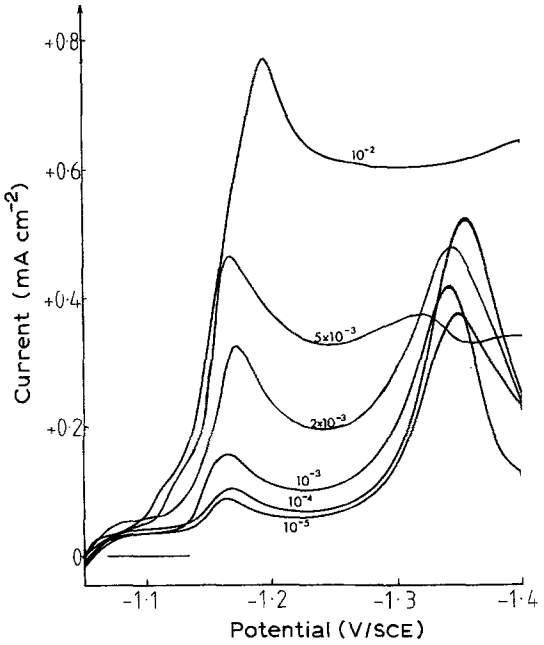

Fig. 2. Voltammograms recorded in deoxygenated 0.2 M $LiClO_4$ containing various concentrations of $Zn(ClO_4)_2$, after holding the potential at -1.15 V for 5 min. Concentrations of $Zn(ClO_4)_2$: 10^{-5}, 10^{-4}, 10^{-3}, 2×10^{-3}, 5×10^{-3}, 10^{-2} M (shown on curves).

~ -1.34 V. Further discussion of O_2 effects follows at the end of this section.

To assign the reverse peaks, the Zn electrode (after 20 min precathodizing at -1.4 V) was scanned from -1.05 V (after being held there for 5 min) to -1.40 V in various $[Zn^{2+}]$ in 0.2 M $LiClO_4$, Fig. 2. The sequence of the -1.15 V peak sizes followed $[Zn^{2+}]$, thus we infer Zn^{2+} aquo-ion reduction, though the Zn^{II} oxide substrate precluded a simple current/concentration relationship. The peak size at -1.3 V did not at all correlate with $[Zn^{2+}]$ undoubtedly because in the pre-treatment conditions required, non-reproduced pre-scan amounts of Zn^{II} oxide were present.

With 0.2 M NH_4ClO_4 in place of $LiClO_4$, the reverse feature at -1.3 V is absent (Fig. 1 inset), and the charge associated with that at -1.15 V increases more markedly with Q_A, Table 1 (Q_A is the *total* anodic charge passed, for both forward and reverse directions). The weakly acidic NH_4^+ in the double layer is said [20] to inhibit the formation of Zn^{II} oxide film on zinc unless the bulk pH is increased to >8.6. The NH_4ClO_4 deletion of the feature observed at -1.3 V in 0.2 M $LiClO_4$ thus suggests that this peak is due to the reduction of a layer of Zn^{II} oxide. The increase in size (NH_4^+ present) with increasing Q_A of the reverse peak at -1.15 V shows that Zn^{II} oxide film in 0.2 M $LiClO_4$ (NH_4^+ absent) has an inhibiting effect on Zn^{2+} reduction. The enhanced forward anodic current in NH_4^+ also betokens weakened Zn^{II} oxide inhibition of Zn^{2+} production in this mileu.

Table 1. Total anodic charge Q_A passed, and charge associated with the cathodic peak at -1.15 V $Q_{-1.15}$ in the reverse limb after long precathodisation (pH 4.6, scan rate 2 mV s^{-1})

	Q_A ($mC\,cm^{-2}$)	$Q_{-1.15}$ ($mC\,cm^{-2}$)
0.2 M NH_4ClO_4	2.7	2.3
	4.3	3.7
	13.7	5.7
	15.2	6.3
0.2 M $LiClO_4$	5.1	0.6
	12.3	0.4
	23.6	0.8

Ellipsometry on the electrode surface during voltammetry shows [4] the formation of a monolayer of ZnO on zinc in neutral $LiClO_4$ from -1.3 V. At yet less negative potential, Zn^{2+} evolves from transfer of Zn^0 through this monolayer. At pH 4.6, incipient hydrogen gas evolution precluded ellipsometry [4], thus a simple diffuse-reflectance technique [18] was used to monitor growth. The forward drift in the reflectance R (Fig. 3a) from -1.4 V to -1.22 V is due to the continuing modification of the electrode surface, stability ensuing only from very long precathodization. The change in slope and subsequent plateau in the CV from -1.25 V to -1.08 V is accompanied by a slight but perceptible decrease in R; the 'reverse' change in R is more marked at the CV peak at ~ -1.33 V (Fig. 3a). Voltammograms of the reverse limb only (Figs 3b and 3c) show the variable nature of the Zn^{II} oxide in that, while the position of the reduction peak in the CV can vary, there is always an

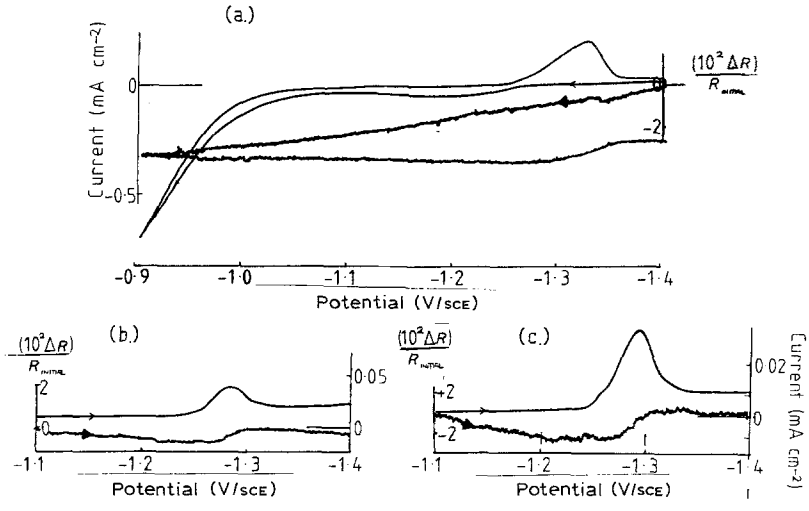

Fig. 3. Voltammograms and reflected light intensities ($10^2 \Delta R/R_{INITIAL}$) for the zinc electrode in 0.2 M $LiClO_4$ after short precathodization. (a) CV reversed at -0.9 V, (b) and (c) reverse limbs only, after sweep reversal at -1.1 V.

Table 2. Total anodic charge Q_A passed, and charge associated with the cathodic peak at -1.3 V, $Q_{-1.3}$ in the reverse limb after use of the various electrode pretreatments in 0.2 M $LiClO_4$ (pH 4.6, scan rate 2 mV s^{-1})

Pretreatment	Q_A ($mC\,cm^{-2}$)	$Q_{-1.3}$ ($mC\,cm^{-2}$)
Long precathodisation	0.0	0.1
	20.1	0.6
Short precathodisation	0.0	0.9
	15.9	5.3
Short precathodisation	0.0	1.3
without deoxygenation	23.6	5.5

accompanying, marked, change in R. Other reactions occur in this potential region, e.g. reduction of H^+, but the marked increases in R are confined to the potential region in which the (reverse) reduction peak appears in the CV, hence the change in R can be attributed to the reduction of a Zn^{II} oxide layer at ~ -1.3 V, removal resulting in a more reflective electrode surface.

The total anodic charge Q_A from graphical coulometry, and the charge corresponding to the feature at -1.3 V, depended on pretreatment (Table 2). While the charge for reduction of a ZnO monolayer is 350 $\mu C\,cm^{-2}$ [21], oxygen, or oxide equivalent to 1 $mC\,cm^{-2}$, may be [22] present on a passivated zinc electrode. In our oxygen-free solutions when minimal anodic charge is passed, the (reverse) -1.3 V feature can be attributed to ZnO monolayer reduction. However, as Q_A is increased, the peak at -1.3 V also grows: if the ZnO is still limited to a monolayer at pH 4.6 (*cf.* Hamnett and Mortimer's 'neutral' [4]), reduction of Zn^{2+} aquo-ion could contribute in addition.

The nature of the Zn^{II} oxide layer formed is found to depend on whether there is dissolved oxygen in the electrolyte. Without oxygen, the change in slope between -1.28 V and -1.20 V is slight (Fig. 1c), and the onset of anodic current occurs in the region -1.10 V to -1.00 V. With oxygen present the forward feature at -1.28 V is more pronounced, and the onset of anodic current is delayed until -0.95 V *cf.* -1.1 to -1.0 V (Fig. 1d, *cf.* Fig. 1c). The Zn^{II} oxide layer is clearly affected by changes in the local chemistry at the electrode surface due to the oxygen reduction. Differing interpretations have been given [6a, 6b] as to whether two successive 2-electron steps with H_2O_2 intermediate, or one overall process governed by $ZnO/Zn(OH)_2$ compositions, is responsible. It suffices here that the Zn^{II} oxide formed is sensitive to milieu including oxygen.

3.2. *Addition of NaH_2PO_4*

Passivating layers comprise ZnO plus $Zn_3(PO_4)_3$ at higher pH [23], in high concentrations of NaH_2PO_4 [24]: the precipitation of $Zn_3(PO_4)_2$ [24] heals breaches in an initially formed layer of ZnO. In our experiments on the addition of NaH_2PO_4 (0.045 M) to 0.2 M $LiClO_4$ at the lower pH 4.6, however, passivation is not observed, NaH_2PO_4 leading to the formation of a *less* passivating oxide layer, as indicated on CVs after each of the three precathodization treatments (Figs. 4a to e) as follows.

After 60 min precathodization (Fig. 4a), the high initial current is attributed [25] to low concentration $H_4PO_4^+$ (from auto-ionisation of H_3PO_4) supposedly more readily reduced than H_3O^+ [25] (actually a greater reducibility to H_2 than H_3O^+ of any of the protonated phosphate species would suffice.) The forward slope change, before onset of anodic current, is more pronounced than in the absence of NaH_2PO_4 (Figs 5a and b, *cf.* Fig. 1b), giving a milky white surface layer. On reversal, only a very slight feature can be seen in the region of -1.3 V. As Q_A is increased (Fig. 4b) a reverse peak develops in the region of -1.16 V, but the feature at -1.3 V remains small, or is hidden by large contributions due to the evident reduction of hydrogen ions (as H_3O^+ or $H_4PO_4^+$ etc): bubbles are observed to form during the reverse limb but not the forward, thus hydrogen gas evolution is a consequence of an activation of the electrode late in the forward sweep (also evidenced by the much larger reverse anodic current for Zn^{2+} evolution, Fig. 4b).

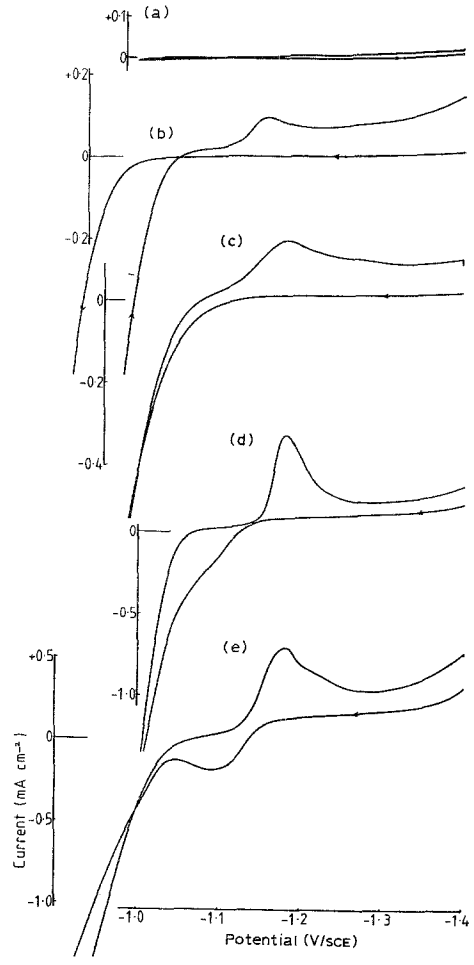

Fig. 4. CVs recorded in 0.2 M $LiClO_4$, 0.045 M NaH_2PO_4: (a) long precathodization. Sweep reversed at -1.0 V; (b) long precathodization. Sweep reversed at -0.9 V; (c) short precathodization. Sweep reversed at -0.95 V; (d) short precathodization without deoxygenation. Sweep reversed at -1.0 V; and (e) short precathodization without deoxygenation. Sweep reversed at -0.9 V.

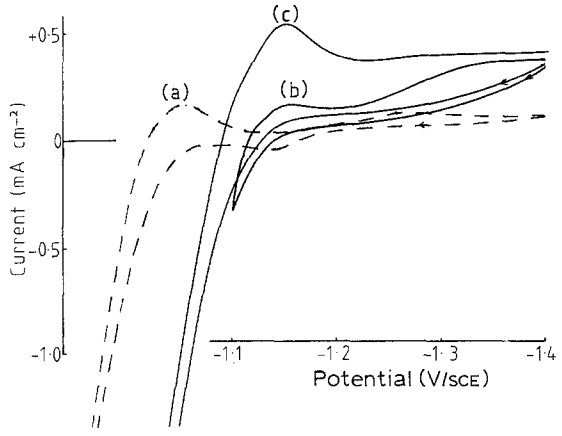

Fig. 5. CV of the zinc electrode in 0.2 M $LiClO_4$, after short pre-cathodization without deoxygenation: (a) in 8.9×10^{-4} M EDTA (disodium salt); (b) and (c) in 0.02 M malic acid with sweep reversed at -1.1 V for (b) and -1.0 V for (c).

Precathodisation for 20 min (Fig. 4c) gives a similar initial cathodic current but the Zn^{II} oxide formed seems already activated, from the earlier forward anodic-current onset. Thus 20 min pre-cathodisation appears not to remove all potentially reactive sites from the electrode surface, whereas the 60 min treatment might.

With oxygen present (Fig. 4d,e) the forward limb shows an extra feature around -1.1 V, either as a slight shoulder (Fig. 4d) or a pronounced peak (Fig. 4e). The large reverse peak observed at -1.2 V has a shoulder at -1.24 V if the extra forward peak is pronounced.

The markedly more negative anodic-onset potential in NaH_2PO_4 (*cf.* -0.95 V, Fig. 1d) indicates a weakening, or diminished, formation of Zn^{II} oxide. In addition, the usual reverse feature at -1.3 V is replaced by one at -1.2 V: a white film does form on the electrode. Furthermore, enhancement of the minute forward step preceeding the anodic-current onset shows that $H_2PO_4^-$ inhibition of Zn^{II} oxide formation promotes dissolution of the metal.

3.3. *Addition of EDTA (disodium salt)*

EDTA (8.9×10^{-4} M) behaves somewhat as NaH_2PO_4, especially with air-exposed solutions. Anodic current onset occurs at -1.16 V. (Fig. 5a), followed by a small peak at -1.13 V then passivity until anodic current flow at -1.08 V. On reversal a peak arises at -1.05 V, with a small plateau at -1.26 V. Deoxygenated electrolytes show the disappearance of the reverse (Zn^{II} oxide) feature normally present at -1.3 V, leaving only a broad peak around -1.05 V, providing clear evidence that EDTA hinders formation of oxide (as is clearly established at pH 9 [6(b)]). However, a white layer does form if oxygen is present, indicating less than total inhibition here by EDTA. Combination of $E^\theta(Zn^{2+}, Zn)$ [19, 26] with stability constants for complex formation at pH 4.6 [27] gives the E^θ value for:

$$Zn(EDTA)^{2-} + 2e^- + \bar{n}H^+ = Zn + H_{\bar{n}}EDTA^{(4-\bar{n})-}$$

for pH 4.6 as -1.275 V with respect to SCE. Absence of a peak at this potential (in deoxygenated solution) shows that the complex is not the electroactive species, and the small reverse peak at -1.26 V (O_2 present) is due to reduction of Zn^{II} oxide. The peak at -1.05 V, apparent only after substantial $Q_A \sim 20$ mC cm^{-2}, can be attributed to Zn^{2+} reduction (*cf.* E^θ $(Zn^{2+}, Zn)_{SCE}$ -1.012 V at ionic strength 0.2 M [19, 26]). The $H_nEDTA^{(4-n)-}$ species are surmised to act as a bridging agent (with an effect like mediation), absence of which imposes a ~ 0.1 V overpotential, as in the -1.15 V reduction of Zn^{2+} (section 3.1).

Addition of 0.1 M EDTA to 0.1 M NaOAc at pH 9 completely inhibits the formation of ZnO film [6(b)], but as the species present are pH dependent [27], the formation of Zn^{II} oxide is clearly only partially inhibited by the particular EDTA species here at pH 4.6.

3.4. *Addition of malic acid*

Malic acid, included in the conversion solution to adjust its pH, induces a higher initial current after each of the precathodization treatments. In all cases, the reverse peak attributed to reduction of Zn^{II} oxide in the region of -1.3 V is absent: malic acid molecules, entrained or adsorbed in the double layer, appear to inhibit the formation of Zn^{II} oxide. In oxygen-

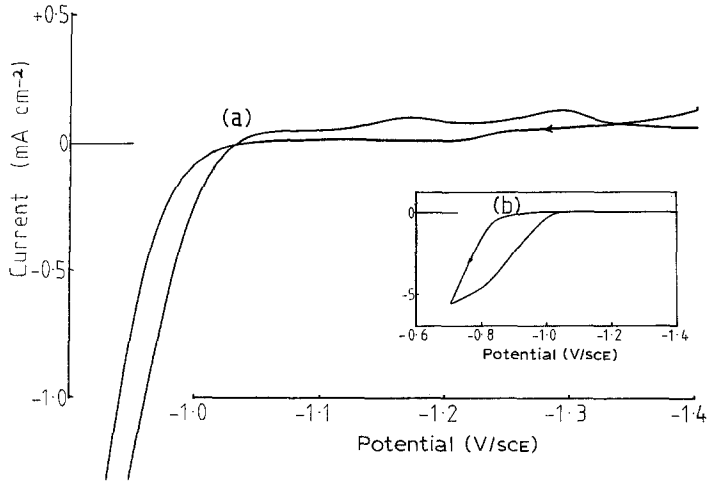

Fig. 6. CV of the zinc electrode in 0.2 M $LiClO_4$, 2.5×10^{-4} M 1-ethoxysulphosuccinic acid: (a) short precathodization without deoxygenation. Sweep reversed at -0.9 V; and (b) long precathodization. Sweep reversed at -0.7 V.

Table 3. Summary of the effects of addition of minor components on the cathodic features observed in the reverse limb

Additive	*Pretreatment*	*Cathodic peak −1.15 V*	*Cathodic peak −1.3 V*
$LiClO_4$ (alone)	(i), (ii), (iii)	Small, little increase with Q_A	Approx 1 monolayer, increases with Q_A
NH_4ClO_4 (alone)	(ii)	Increases with Q_A	Absent
NaH_2PO_4	(i), (ii), (iii)	Increases with Q_A	Very small, masked by H^+ reduction current
EDTA	(ii)	Increases with Q_A	Absent
	(iii)	Increases with Q_A	Small feature
Malic acid	(i), (ii), (iii)	Increases with Q_A	Absent
1-ethoxysulphosuccinic acid	(ii)	Absent	Absent
	(iii)	Small, little increase with Q_A	Smaller than in $LiClO_4$ alone

containing solutions no inhibition of electrode dissolution is seen. Anodic onset occurs at −1.13 V, beyond which current increases rapidly (Figs 5b and 5c), while in the reverse, the Zn^{2+} reduction appears at the usual −1.15 V, beyond which a substantial current plateau is observed. As Q_A is increased the −1.15 V peak increases in size and the plateau begins at more positive potential. The inferred absence of Zn^{II} oxide accounts for these observations.

3.5. *Addition of the surfactant, 1-ethoxysulphosuccinic acid (A102), and of the humectant, isopropanol*

The pretreatment is important again. In oxygen-containing solutions A102 has an inhibiting effect on ZnO formation, resulting in a less passivating film. Thus the forward cathodic-current step and the subsequent plateau are as observed without A102, but the plateau does not extend to such positive potential, and anodic onset occurs at −1.03 V (Fig. 6a) as opposed to −0.95 V (Fig. 1d). *Less* ZnO is formed − a smaller peak is observed in the reverse at −1.3 V than is observed in 0.2 M $LiClO_4$ alone, in addition to the usual Zn^{2+} reduction peak at −1.16 V.

After 60 min precathodization, A102 also has an inhibiting effect on the other electrode reactions: while onset of anodic dissolution falls in the usual range −1.02 V to −0.96 V, the absence of *any* reverse features shows that the re-reduction of zinc ion is effectively suppressed, even if a large Q_A is passed, up to 700 mC cm^{-2} (Fig. 6b). These observations imply exceptionally strong adsorption of the surface active agent at the electrode interface, which partially insulates the surface.

The humectant IPA has no effect on the electrochemistry, which accords well with its assigned role as prevention of solution dry-out during use of the commercial fluid.

4. Conclusions

The variable-composition zinc oxide/hydroxide film forms observably at ~ −1.2 V in the negative-to-positive limb of the CV and affects both the anodic formation of Zn^{2+}, its re-reduction in the reverse limb and its own re-reduction. Long pre-cathodisation of the Zn electrode inhibits both the formation of the layer and of Zn^{2+}.

In the reverse limb peaks at ~ −1.15 V and −1.3 V are ascribable to reduction of Zn^{2+} and of the oxide/hydroxide film, respectively. NH_4^+ precludes formation of the film.

The effect of minor constituents is summarized in Table 3, the surfactant preventing both cathodic processes. NaH_2PO_4 and malic acid are thought to inhibit the formation of ZnO in much the same way as has been reported for the NH_4^+ ion, by decreasing the local pH at the electrode surface; no peak appears for EDTA complexes with Zn^{II}. The inhibitions attributed to the surface active agent A102 are ascribed to its strong adsorption at the electrode surface.

Acknowledgements

We thank the SERC and Gestetner Manufacturing Ltd (GML) for the award of a CASE studentship to A.M.S., and GML for support of J.D.S. We are indebted to Dr R. J. Mortimer for preliminary experiments and advice, to Mr D. McGee for valuable discussions and to Dr J. B. Jackson for defining the problem and for continued support.

References

[1] R. M. Schaffert, 'Electrophotography', 2nd Edn., Focal Press, London (1980).
[2] M. Kuzuwata, H. Machida, H. Tamura and T. Saito, Ricoh Co. Ltd, U.S. Pat. 4 208 212 (1980).
[3] S. Shimizu and T. Tanno, British Pat. No. 1 229 052 (1971).
[4] A. Hamnett and R. J. Mortimer, *J. Electroanal. Chem.* **234** (1987) 185.
[5] L. M. Baugh, *Electrochim. Acta* **24** (1979) 657.
[6] (a) C. Deslouis, M. Duprat and C. Tulet-Tournillon, *J. Electroanal. Chem.* **181** (1984) 119; (b) K. G. Boto and L. F. G. Williams, *J. Electroanal. Chem.* **77** (1977) 1.
[7] A. Hugot-Le Goff, S. Joiret, B. Saïdani and R. Wiart, *ibid.* **263** (1989) 127.
[8] R. W. Powers and M. W. Breiter, *J. Electrochem. Soc.* **116** (1969) 719.
[9] G. S. Bell, *Electrochim. Acta* **13** (1968) 2197.
[10] M. N. Hull and J. E. Toni, *Trans Faraday Soc.* **67** (1971) 1128.
[11] R. D. Armstrong, G. M. Bulman and H. R. Thirsk, *J. Electroanal. Chem.* **22** (1969) 55.
[12] K. Huber, *J. Electrochem. Soc.* **100** (1953) 376.
[13] M. C. H. McKubre and D. D. McDonald, *ibid.* **128** (1981) 524.

[14] M. Pourbaix, 'Atlas of Electrochemical Equilibria In Aqueous Solution', Pergamon Press, Oxford (1966) p. 113.
[15] C. Deslouis, M. Duprat and C. H. R. Tournillon, *Corros. Sci.* **29** (1989) 13.
[16] C. Cachet and R. Wiart, *J. Electroanal. Chem.* **129** (1981) 103; I. Epelboin, M. Ksouri and R. Wiart, *Faraday Symp. Chem. Soc.* **12** (1978) 115.
[17] F. Berthier, J. P. Diard, B. Le Gorrec, C. Montella and P. Landaud, Extended Abstracts, 1st International Symposium on Electrochemical Impedance Spectroscopy, Bombannes (1989) C1.9.
[18] D. R. Rosseinsky, J. D. Slocombe, A. M. Soutar, P. M. S. Monk and A. Glidle, *J. Electroanal. Chem.* **258** (1989) 233.
[19] A. M. Soutar, Ph.D. Thesis, Exeter (1990).
[20] L. M. Baugh, *Electrochim. Acta* **24** (1979) 669.
[21] R. D. Armstrong, G. M. Bulman and H. R. Thirsk, *J. Electroanal. Chem.* **22** (1969) 55.
[22] B. N. Kabanov, *Electrochim. Acta* **6** (1962) 253.
[23] C. P. DePauli, O. A. H. Derosa and M. C. Giordano, *J. Electroanal. Chem.* **73** (1976) 105.
[24] C. Cachet, C. P. DePauli and R. Wiart, *Corros. Sci.* **25** (1985) 493.
[25] S. A. Awad and Kh. M. Kamel, *J. Electroanal. Chem.* **24** (1970) 217.
[26] C. Berecki-Biederman, G. Biederman and L. G. Sillén, 'Report to Analytical Section IUPAC: Zn, Cd, Hg Potentials', IUPAC (1953).
[27] C. L. Wilson and D. W. Wilson, 'Comprehensive Analytical Chemistry', Vol. **1B**, Elsevier, Amsterdam (1960) p. 299.